Electronic Supplementary Material (ESI) for RSC Advances.

Supplementary Information

Additive-free photo-mediated oxidative cyclization of pyridinium acylhydrazones to 1,3,4-oxadiazoles: solid-state conversion in a microporous organic polymer and supramolecular energy-level engineering

*Kyung-su Kim, You Kyoung Chung, Hyun Woo Kim, Chae Yeon Ha Joonsuk Huh, and Changsik Song**

Department of Chemistry, Sungkyunkwan University, 2066 Seobu-ro, Janan-gu, Suwon-si, Gyeonggi-do 16419 Republic of Korea.

Email: songcs@skku.edu

Supporting Figures

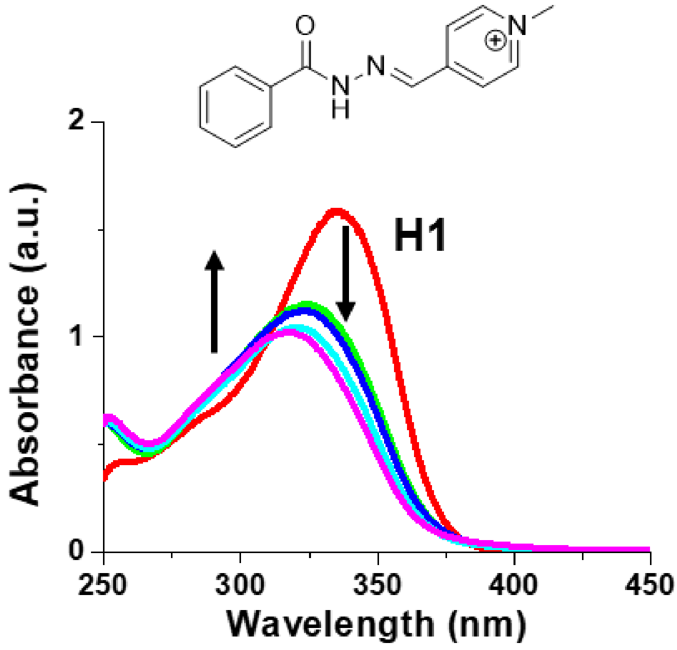

Fig. S1. UV-Vis spectra of **H1** upon irradiation of UV-light with 342 nm (0.66 mM in DMSO).

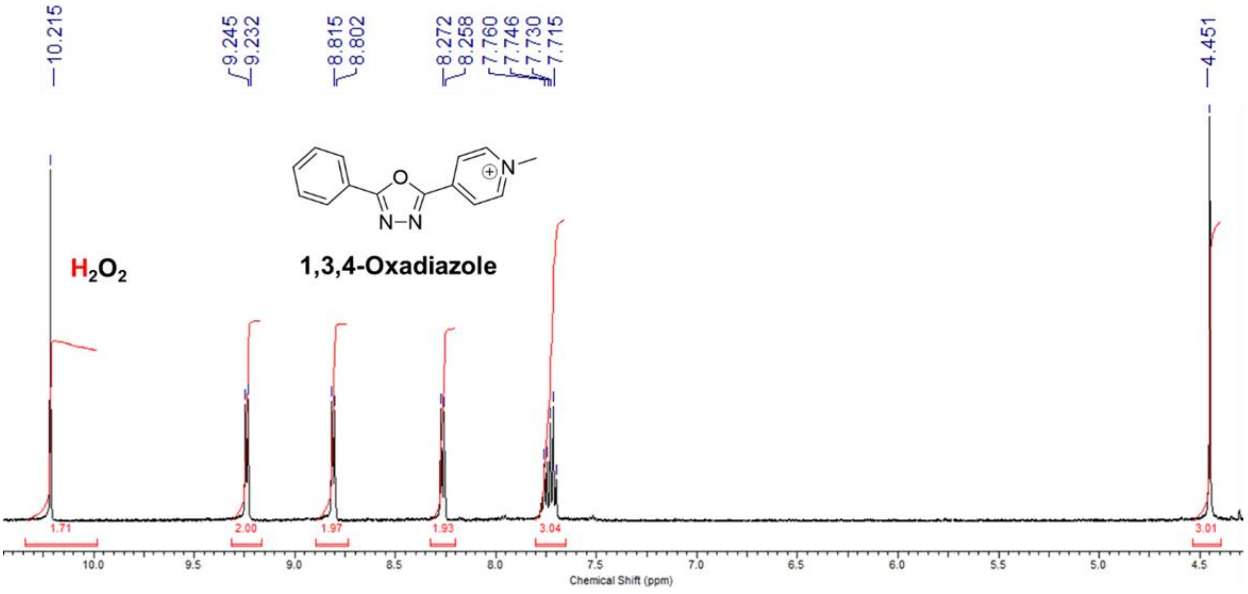

Fig. S2. ^{1}H-NMR spectrum of the reaction mixture of H1 (0.66 mM) after UV irradiation (342 nm, 1.5 h) to produce 2-methylpyridinium-5-phenyl-1,3,4-oxadiazole (700 MHz, DMSO-d_6).

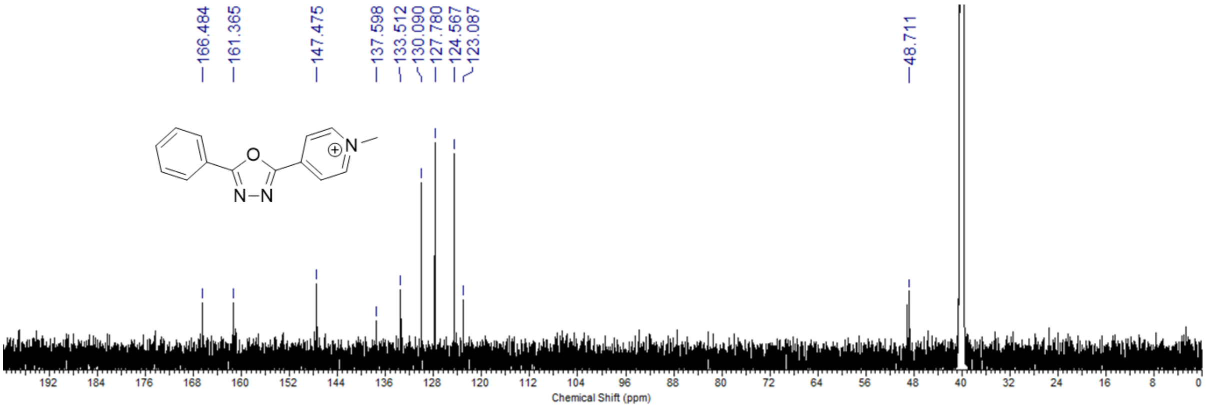

Fig. S3. ^{13}C-NMR spectrum of 2-methylpyridinium-5-phenyl-1,3,4-oxadiazole (175 MHz, DMSO-d_6).

HRMS (ESI+) [$C_{14}H_{12}N_3O$]: calcd [M]$^+$ 238.0975, found: 238.0975

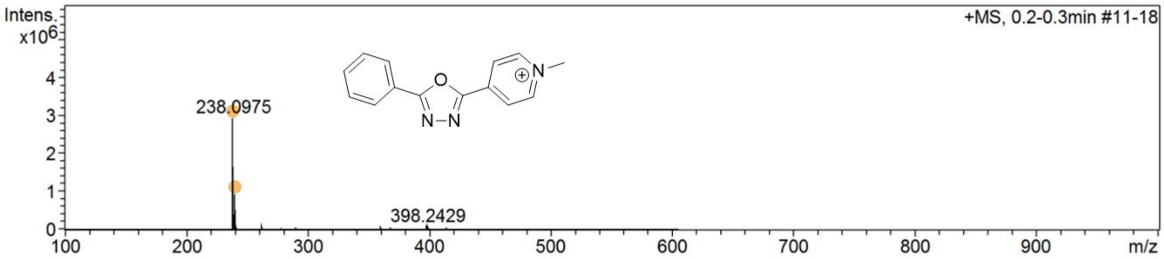

```
Meas. m/z   #   Ion Formula        m/z   err [ppm]   mSigma   # Sigma    Score   rdb   e⁻ Conf   N-Rule
 238.0975   1   C14H12N3O     238.0975         0.1     16.3         1   100.00  10.5   even          ok
            1   C12H13N3NaO   238.0951        10.0      6.8         1   100.00   7.5   even          ok
```

Fig. S4. HRMS-ESI spectrum of 2-methylpyridinium-5-phenyl-1,3,4-oxadiazole.

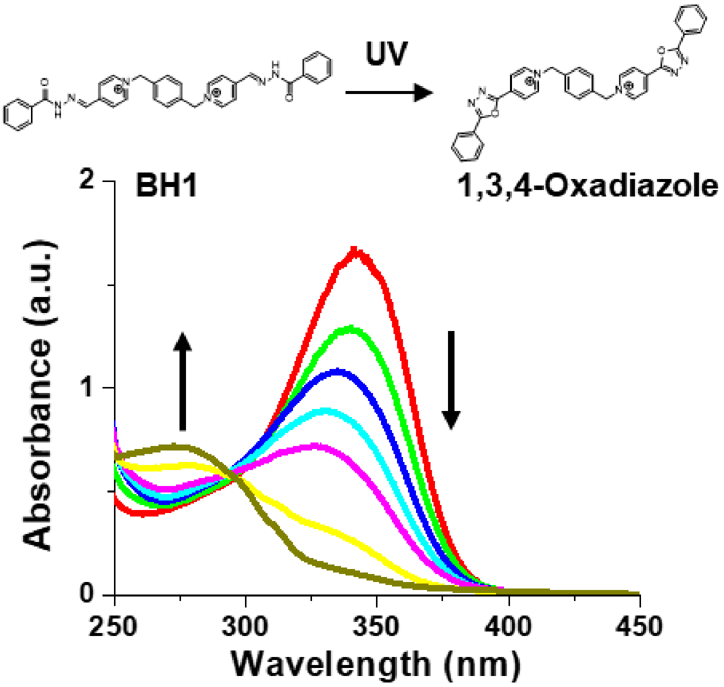

Fig. S5. UV-Vis spectra of **BH1** (0.33 mM in DMSO) upon UV light irradiation (342 nm). The black arrows indicate the direction of change in absorbance as the irradiation time increases.

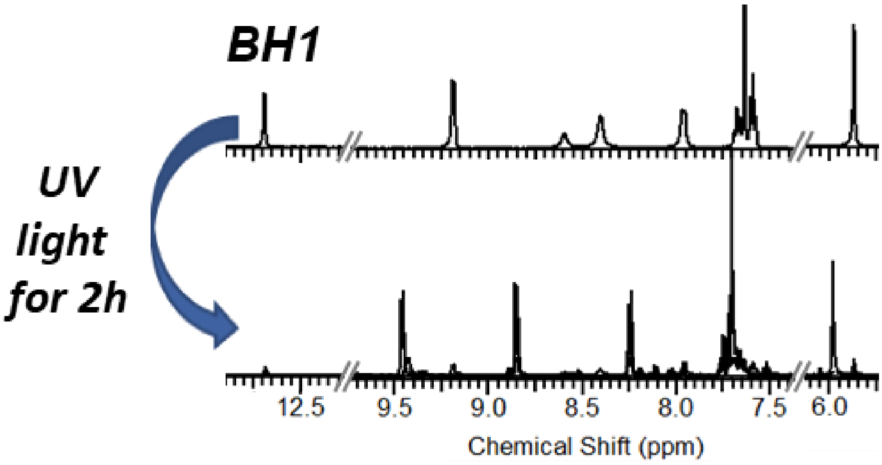

Fig. S6. ^{1}H NMR spectra of **BH1** before and after UV-irradiation (342 nm) for 2 h (500 MHz, 0.33 mM in DMSO).

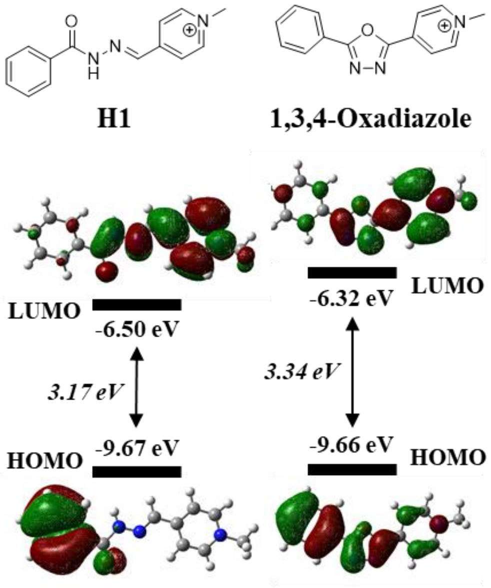

Fig. S7. Calculated lowest unoccupied molecular orbital (LUMO) and highest occupied molecular orbital (HOMO) orbitals and the energy levels of **H1** (left) and 1,3,4-oxadiazole (right).

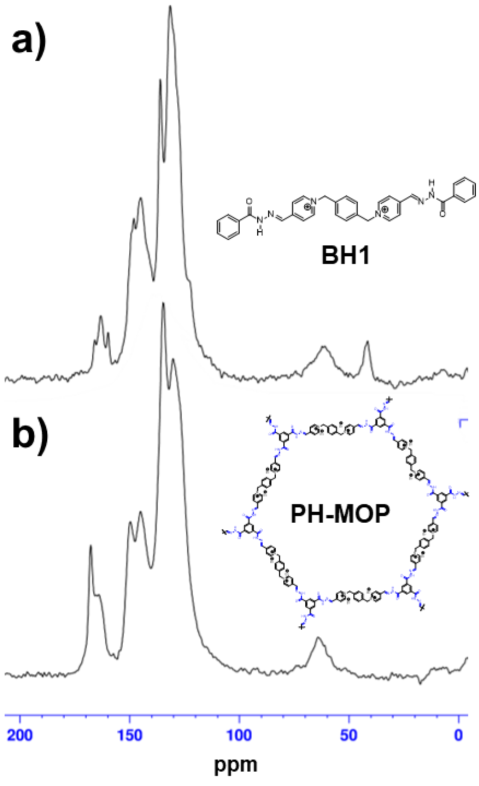

Fig. S8. Solid-state ^{13}C CP-MAS NMR of **BH1** (a) and **PH-MOP** (b).

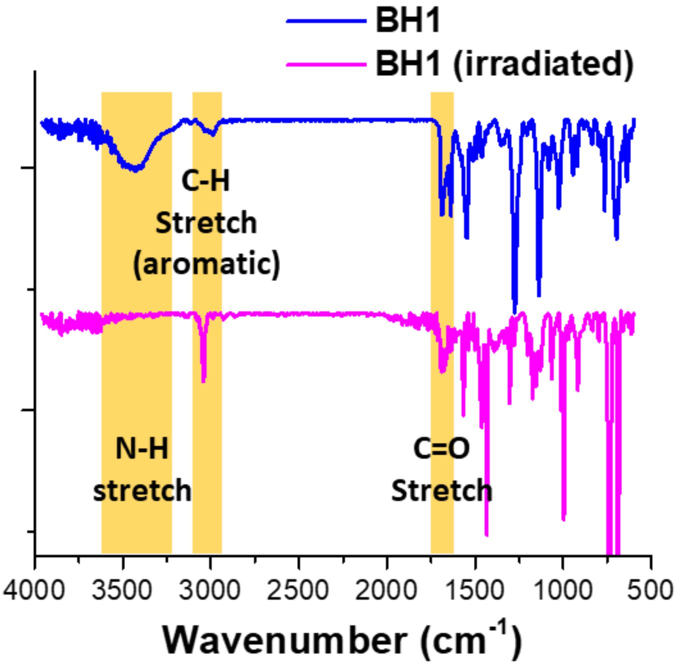

Fig. S9. FT-IR spectra of **BH1** before (blue-line) and after (pink-line) UV-irradiation in the solid state.

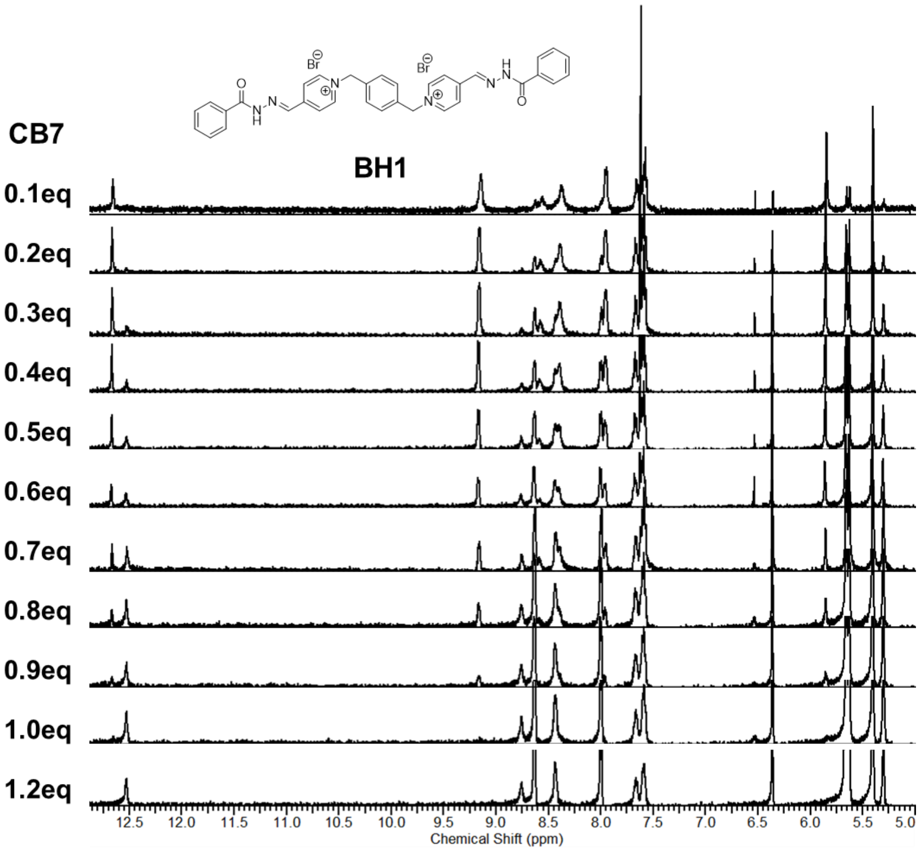

Fig. S10. ^{1}H NMR titration experiment of **BH1** upon addition of **CB7** (1.0 mM in DMSO-d_6).

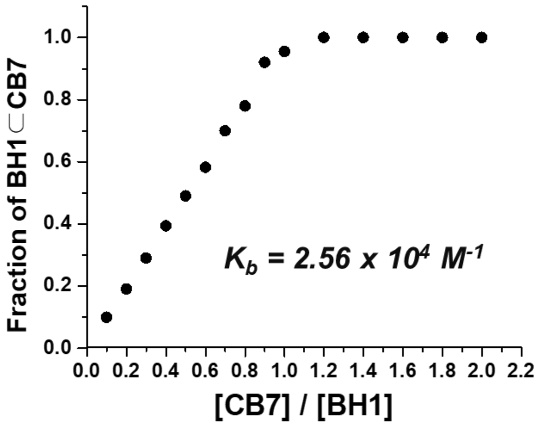

Fig. S11. The plot of the fraction of **BH1⊂CB7** versus **CB7** (obtained from NMR titration experiments).

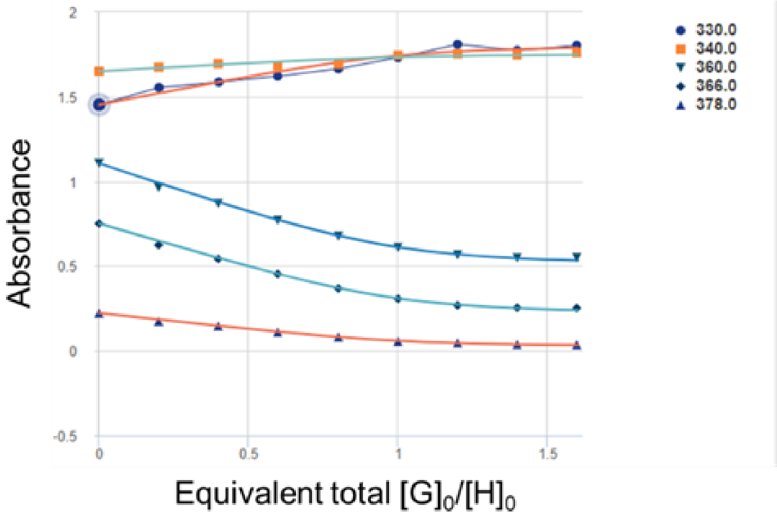

$$\mathrm{H} + \mathrm{G} \overset{K_a}{\rightleftharpoons} \mathrm{HG}$$

$$K_a = \frac{[HG]}{[H][G]}$$

Fig. S12. The fitting to the binding isotherm (1:1) of **BH1** to **CB7** from the absorbance at the wavelengths of 330, 340, 360, 366, and 378 nm. H is the host molecule **CB7** and G is the guest molecule **BH1**. The fitting results were obtained using the website http://supramolecular.org/.

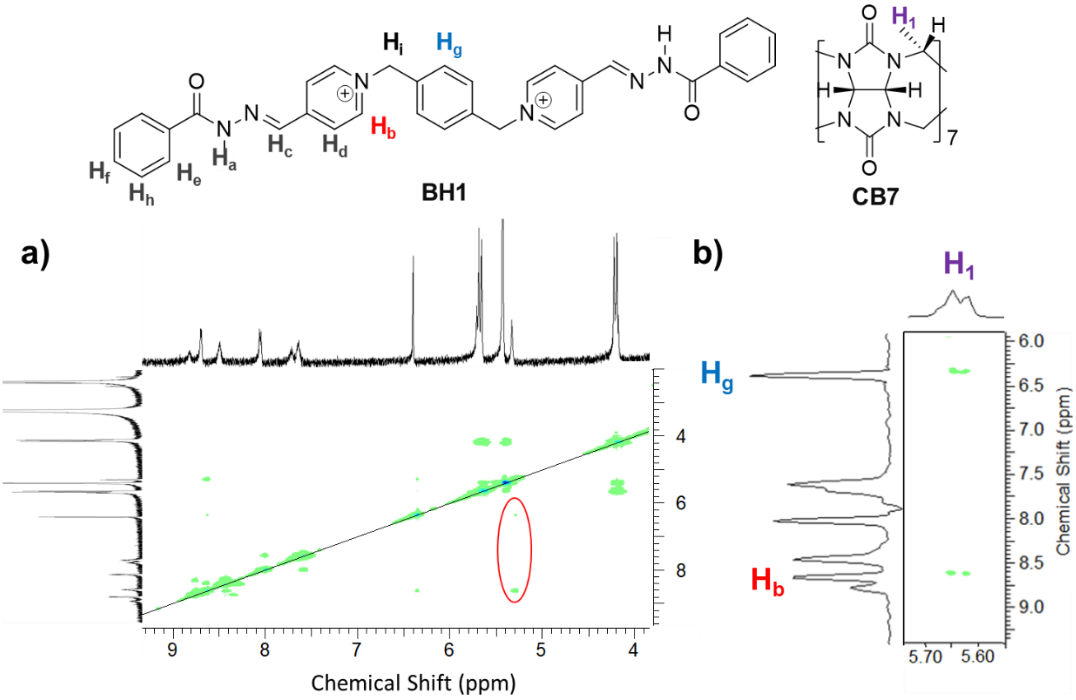

Fig. S13. a) Rotating-frame Overhauser spectroscopy (ROESY) NMR spectrum of **BH1⊂CB7** in DMSO-d_6 (1.0 mM) and b) the selected area for H_1 with H_b and H_g.

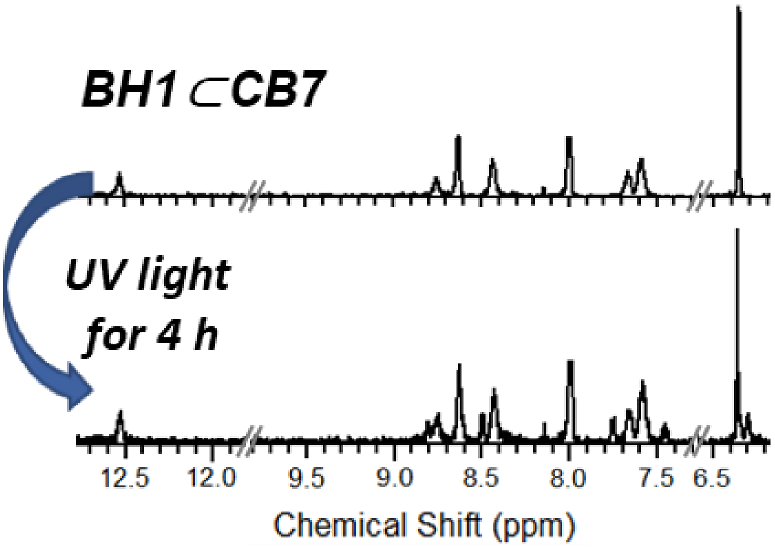

Fig. S14. Selected ^{1}H NMR spectra of **BH1⊂CB7** before and after irradiation with 342-nm UV light for 4 h (500 MHz, 0.33 mM in DMSO-d_6).

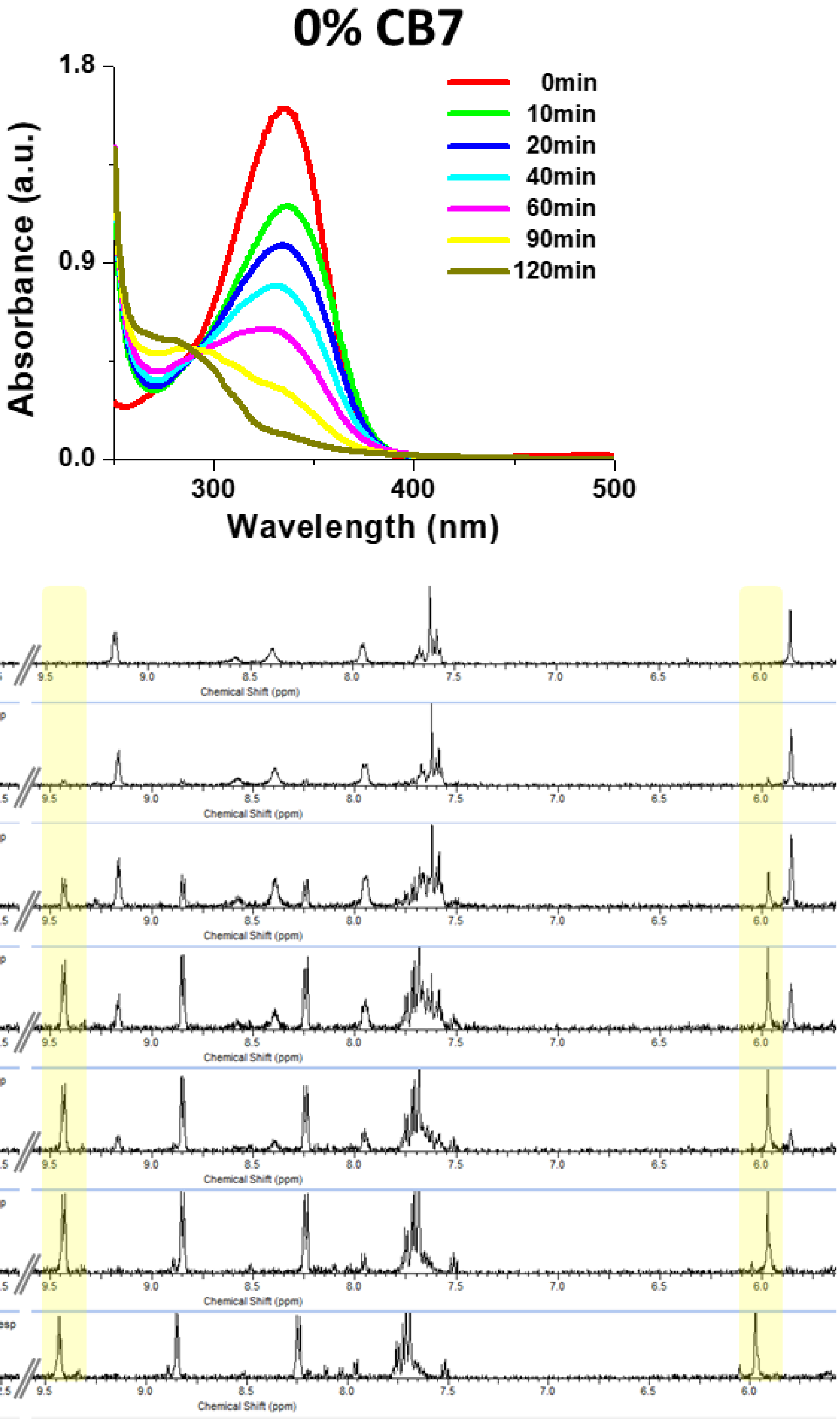

Fig. S15a. The UV-irradiation time-dependent UV-Vis spectra and NMR spectrum of **BH1** with 0% contents of **CB7** (500 MHz, 0.33 mM in DMSO-d_6).

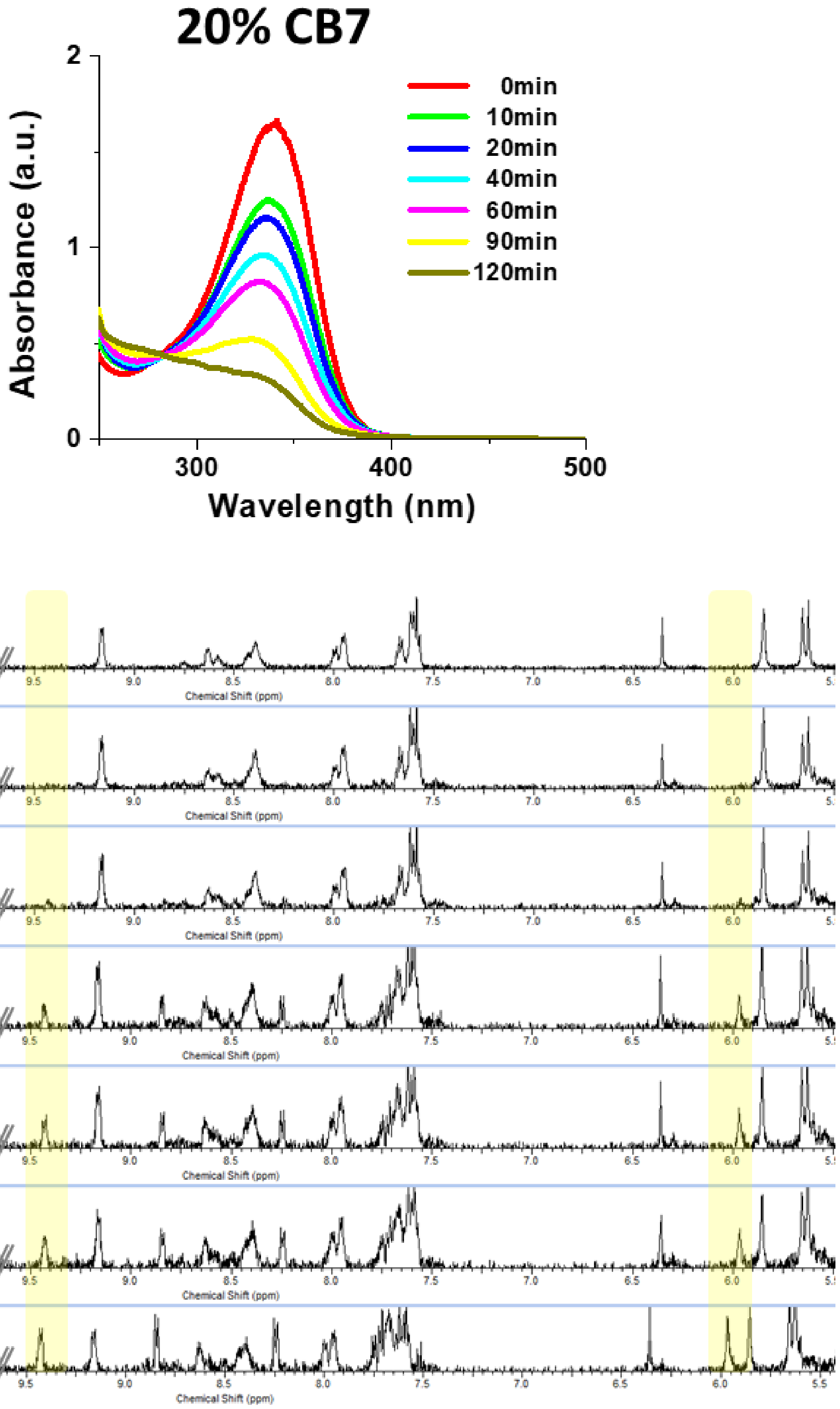

Fig. S15b. The UV-irradiation time-dependent UV-Vis spectra and NMR spectrum of **BH1** with 20% contents of **CB7** (500 MHz, 0.33 mM in DMSO-d_6).

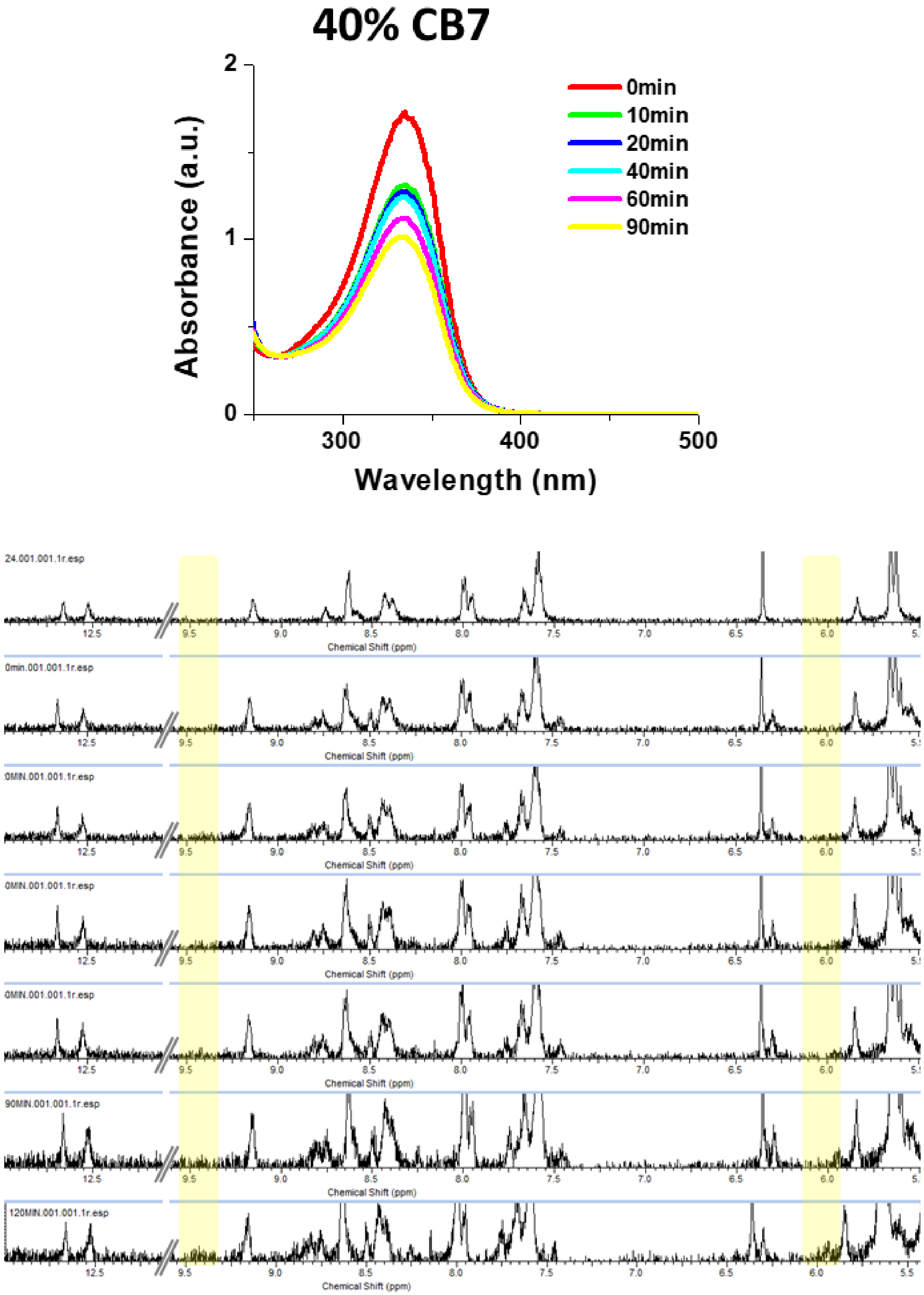

Fig. S15c. The UV-irradiation time-dependent UV-Vis spectra and NMR spectrum of **BH1** with 40% contents of **CB7** (500 MHz, 0.33 mM in DMSO-d_6).

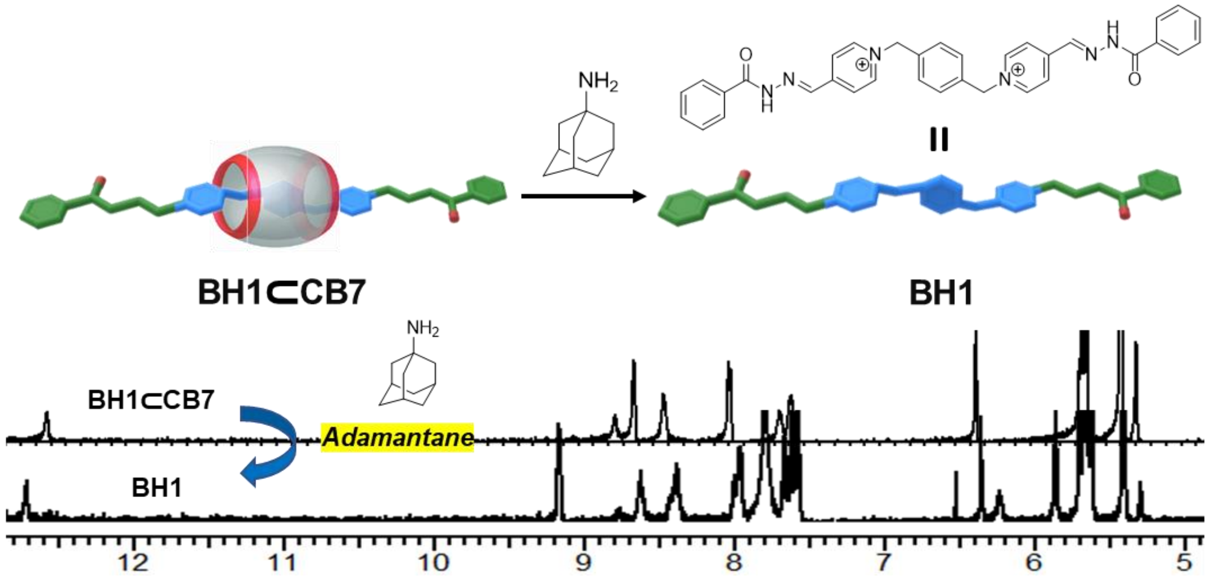

Fig. S16. ^{1}H NMR spectra of inclusion complexes, **BH1⊂CB7** (500 MHz, 1.0 mM in DMSO-*d*$_6$) upon addition of 1-adamantanamine.

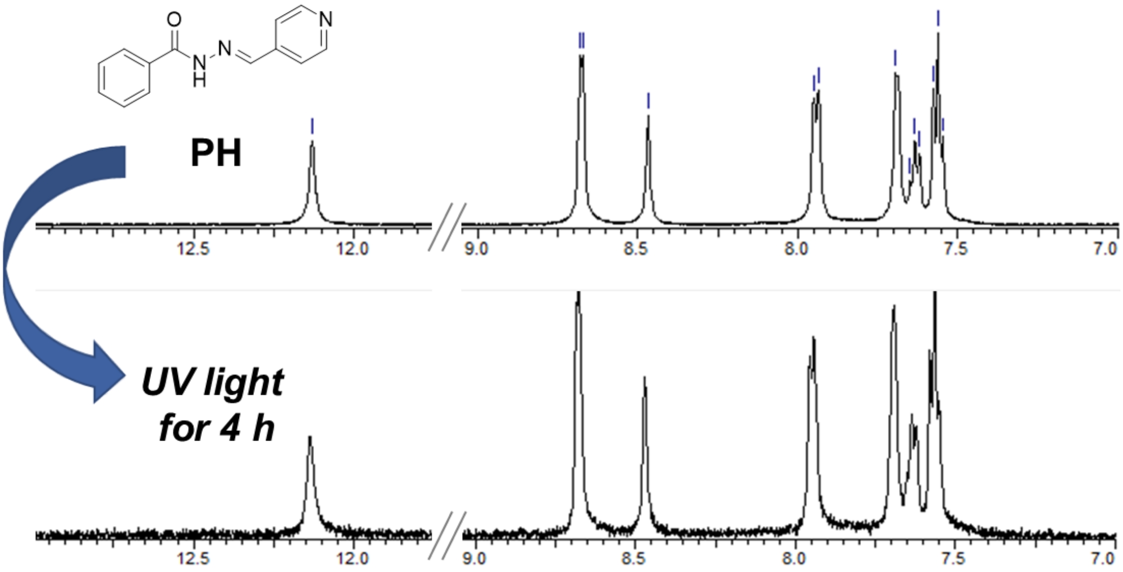

Fig. S17. UV irradiation (342 nm) time-dependent ^{1}H NMR spectra for pyridine acylhydrazone conjugate, **PH** (500 MHz, 0.66 mM in DMSO-*d*$_6$).

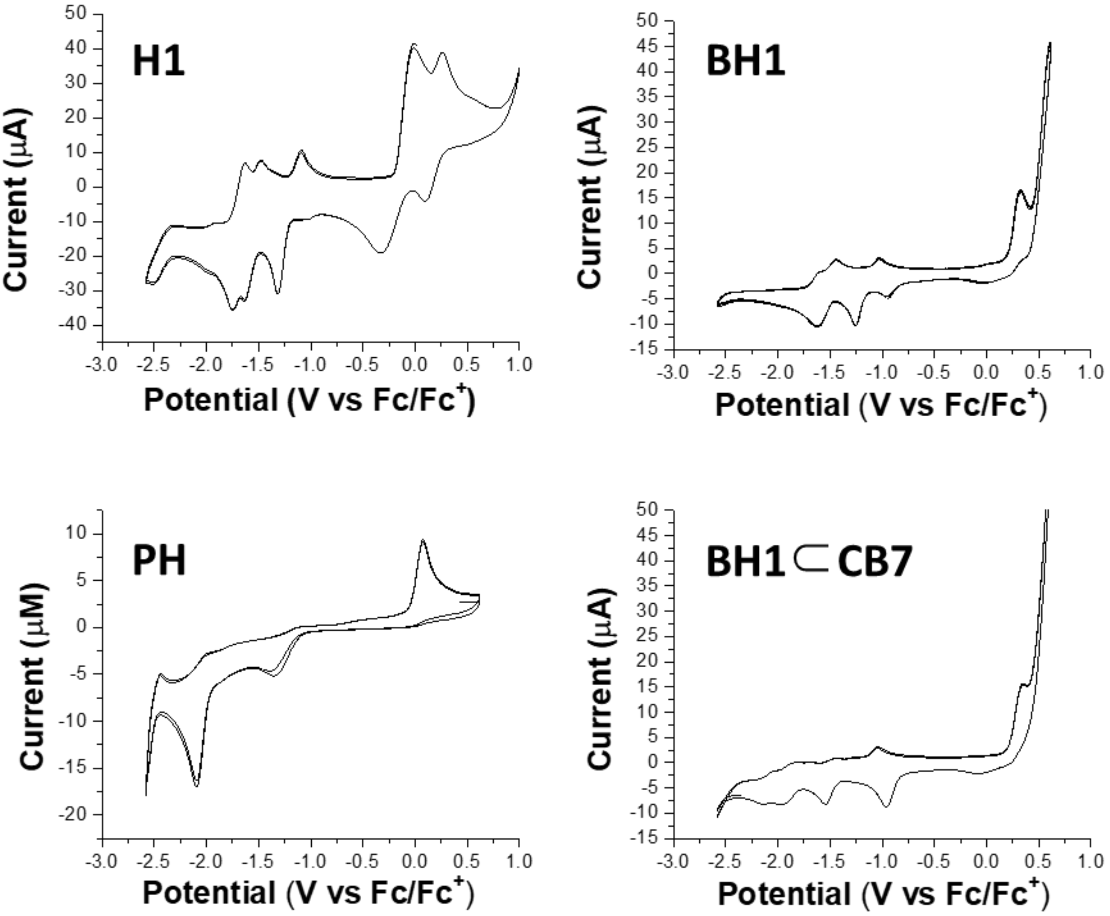

Fig. S18. Cyclic voltammograms of **H1**, **PH**, **BH1**, and **BH$\subset$CB7** in DMSO (1.0 mM) with 0.1 M tetrabutylammonium hexafluorophosphate ($TBAPF_6$) as a supporting electrolyte in a three-electrode cell configuration (a quasi-internal Ag wire reference electrode submerged in 0.01 M $AgNO_3$/0.1 M $TBAPF_6$ in anhydrous CH_3CN, a 1.6-mm Pt button working electrode, and a Pt coil counter electrode). The initial potential was set at -0.5 V (vs Ag/Ag^+), and all scans were initiated in the negative direction with a scan rate of 100 mV s^{-1}.